

Correlating structure, strain, and morphology of self-assembled InAs quantum dots on GaAs

D. P. Kumah, J. H. Wu, N. S. Husseini, V. D. Dasika, R. S. Goldman et al.

Citation: *Appl. Phys. Lett.* **98**, 021903 (2011); doi: 10.1063/1.3535984

View online: <http://dx.doi.org/10.1063/1.3535984>

View Table of Contents: <http://apl.aip.org/resource/1/APPLAB/v98/i2>

Published by the [AIP Publishing LLC](#).

Additional information on *Appl. Phys. Lett.*

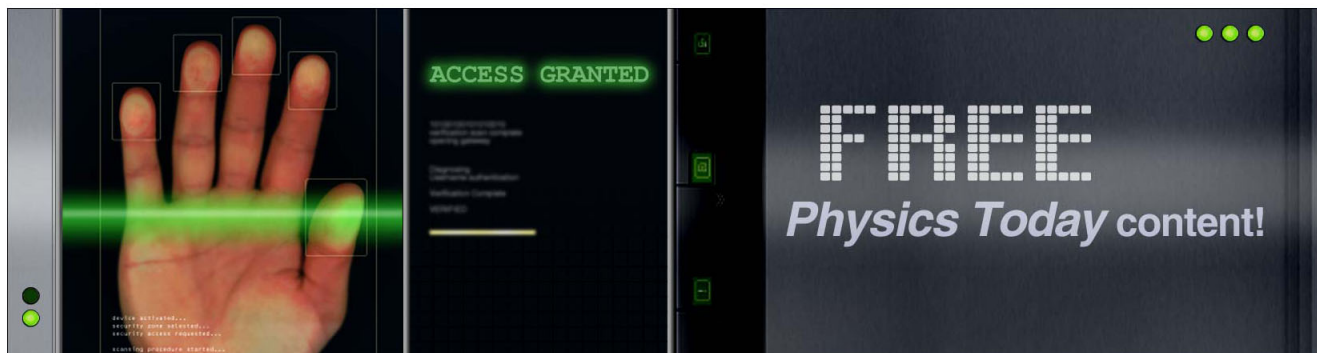
Journal Homepage: <http://apl.aip.org/>

Journal Information: http://apl.aip.org/about/about_the_journal

Top downloads: http://apl.aip.org/features/most_downloaded

Information for Authors: <http://apl.aip.org/authors>

ADVERTISEMENT



Correlating structure, strain, and morphology of self-assembled InAs quantum dots on GaAs

D. P. Kumah,^{1,a)} J. H. Wu,² N. S. Husseini,¹ V. D. Dasika,^{2,3,b)} R. S. Goldman,^{2,3} Y. Yacoby,⁴ and R. Clarke^{1,3}

¹Applied Physics Program, University of Michigan, Ann Arbor, Michigan 48109, USA

²Department of Materials Science and Engineering, University of Michigan, Ann Arbor, Michigan 48109, USA

³Center for Solar and Thermal Energy Conversion, University of Michigan, Ann Arbor, Michigan 48109, USA

⁴Racah Institute of Physics, Hebrew University, Jerusalem 91904, Israel

(Received 19 October 2010; accepted 16 December 2010; published online 11 January 2011)

We report on the use of a direct x-ray phase retrieval method, coherent Bragg rod analysis, to characterize self-assembled InAs quantum dots (QDs) grown epitaxially on GaAs substrates. Electron density maps obtained close to the x-ray absorption edges of the constituent elements are compared to deconvolute composition and atomic spacing information. Our measurements show no evidence of a wetting layer and reveal bowing of the atomic layers throughout the QD, extending from the QD-substrate interface. This leads to a half-layer stacking shift which may act to partially decouple the QDs electronically from the substrate. © 2011 American Institute of Physics. [doi:10.1063/1.3535984]

The spontaneous transition of strained two-dimensional (2D) films into homogeneous three-dimensional (3D) islands, the Stranski–Krastanow growth mode,¹ has attracted much scientific attention. It has led to the realization of self-assembled quantum dot (QD) structures with a wide range of technological applications resulting from the atomlike density of states.² However, many questions still remain in understanding how 3D islands form^{3,4} and the nature and distribution of strain and chemical composition within the resulting QDs.^{5–7}

In this letter, using direct x-ray phase retrieval methods,^{8,9} we present new insights on the internal structure of self-assembled InAs QDs epitaxially grown on GaAs substrates. The layer-by-layer composition and the atomic structure of the QDs, including the QD-substrate interface, are elucidated from 3D electron density maps. The maps were obtained by coherent Bragg rod analysis (COBRA) using x-ray diffraction at energies tuned close to the Ga and As x-ray absorption edges. The energies were selected to enhance chemical sensitivity, by exploiting the energy dependence of the scattering factors of the constituent elements of the system.¹⁰ Our results reveal key aspects of the microscopic structure and morphology that may have an important bearing on their optoelectronic properties. In particular, we present direct structural evidence supporting previous photoluminescence-based claims that the wetting layer is largely consumed by the QDs at high coverage.¹¹ We will also show that the atomic-layer stacking undergoes a half-monolayer shift from the substrate into the QD, accompanied by a bowing of the layers. This observation, together with the fact that there is no observable wetting layer in these high density QD samples, suggests that the QDs so formed are

partially decoupled from the substrate with respect to their low-dimensional optoelectronic properties.

The self-assembled InAs QDs were grown epitaxially on a GaAs buffer layer prepared using a growth and *in situ* annealing sequence described in the supplementary materials.^{12,13} The GaAs buffer contains a high density of nucleation sites consisting of bilayer step-terraces and surface “mounds,”^{13,14} which enabled the formation of a high density ($6.4 \pm 0.3 \times 10^{10}$ dots/cm²) of InAs QDs, with dimensions of 3.8 ± 0.5 nm (height) and 20 ± 5 nm (width), as evidenced by atomic force microscopy (AFM). Cross-sectional scanning tunneling microscopy (XSTM) measurements were obtained on samples grown in a similar manner but capped with GaAs.

Surface diffraction experiments were carried out at the 7-ID and 33-ID undulator beamlines of the Advanced Photon Source, Argonne National Laboratory. Nine symmetry-inequivalent Bragg rods were obtained at 10.362 and 11.862 keV, 5 eV below the Ga and As absorption edges, respectively. The rods measured were the $00L$, $11L$, $1\bar{1}L$, $20L$, $22L$, $31L$, $3\bar{1}L$, $33L$, and $3\bar{3}L$ rods with $L_{\max} = 4.5$ reciprocal lattice units and a sampling density of 40 points per GaAs reciprocal lattice unit.

The diffraction intensities were converted to real space 3D electron density maps using the COBRA algorithm.⁸ The atoms in QDs do not form a strictly 2D periodic array but the atomic positions are registered with respect to the underlying substrate atoms. Therefore the COBRA-derived maps are the electron densities of the “folded” structure,¹⁵ namely, the structure obtained by laterally translating each atom in the system to one substrate-defined 2D unit cell (UC) using substrate-defined 2D UC vectors.

Profiles normal to the surface through the group III (G-III) and V (G-V) lattice sites are shown in Fig. 1 for the data obtained at the two x-ray energies. The nominal QD-substrate interface is located at $z=0$. The larger, narrow peaks for $z < 0$ correspond to the substrate atoms. The

^{a)}Present address: Center for Research on Interface Structures and Phenomena, Yale University, New Haven, CT. Electronic mail: dkumah@umich.edu.

^{b)}Present address: University of Texas at Austin, Austin, TX.

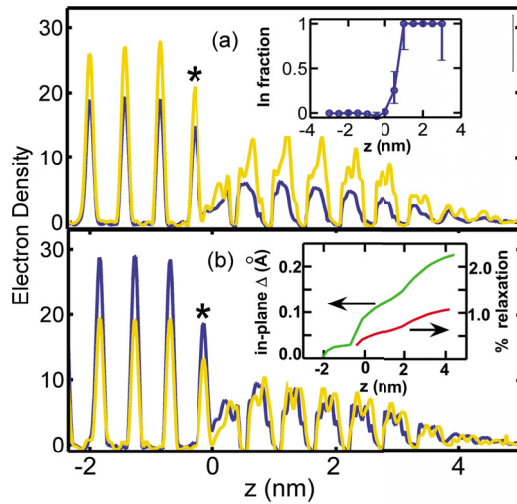


FIG. 1. (Color online) Comparison of vertical electron density profiles through atomic positions for (a) As and (b) Ga (In) from electron density maps obtained from measurements close to the Ga K-edge (light) and the As K-edge (dark). The asterisk denotes fractionally occupied substrate layers. The substrate-QD In concentration profile is shown inset in (a). The profiles of the average in-plane atomic displacement, Δ , and the corresponding in-plane relaxation, are shown inset in (b).

smaller, broader peaks at $z > 0$ correspond to the QD region. The QD peaks are smaller because the QDs occupy only a fraction of the surface. The QD peaks are found to extend to a height of 4 nm, in good agreement with the AFM data.

As expected, the ratio between the integrated electron densities at the two energies through the G-V lattice sites in Fig. 1(a) is equal to the ratio between the As atomic scattering factors at these energies. Similarly, the ratio between the substrate peaks in Fig. 1(b) at $z < 0$ equals the ratio between the Ga scattering cross sections. The narrow peaks just below $z = 0$ (marked with an asterisk) are smaller than the deeper substrate peaks, indicating that the topmost substrate layer is incomplete due to substrate surface roughness. The ratio between this pair of peaks also indicates GaAs stoichiometry demonstrating the absence of a wetting layer. On the other hand, the QD peaks at $z > 0$ in Fig. 1(b) are approximately equal, suggesting that the G-III element in the QDs is In.

The In concentration, ρ_{In} , can be expressed quantitatively in terms of the ratio, R , between peak integrated electron densities measured at the As edge and the Ga edge as follows

$$\rho_{\text{In}} = \frac{R * S_{\text{Ga}}^{\text{Ga}} - S_{\text{Ga}}^{\text{As}}}{(S_{\text{In}}^{\text{As}} - S_{\text{Ga}}^{\text{As}}) - R * (S_{\text{In}}^{\text{Ga}} - S_{\text{Ga}}^{\text{Ga}})}, \quad (1)$$

where, $S_{\text{Ga}}^{\text{As}}$ is the scattering factor of Ga measured at the As edge, etc. The results averaged over the two independent Ga lines are shown inset in Fig. 1(a). The In concentration is bound by unity on the upper side and the asymmetric error bars on the lower side. These results show that, at the interface, the In concentration rises sharply to close to unity within 1–1.5 UCs, while below the interface, it is essentially zero.

The average outer QD shape is also determined from the electron density profiles. The QD width, $w(z)$, can be expressed in terms of the fraction, $\theta(z)$, of the area covered by the QDs obtained from the electron density profiles and the QD density, n , determined from AFM measurements

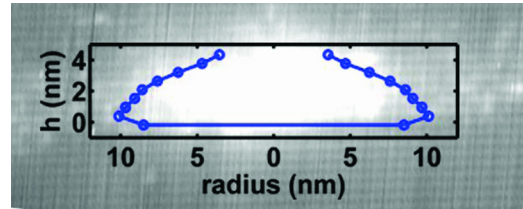


FIG. 2. (Color online) Profile of the individual QD shape drawn to scale as determined by COBRA overlaid on a XSTM image of a buried QD sample.

$$w(z) = \sqrt{\frac{\theta(z)}{n}}. \quad (2)$$

A diagram of the QD shape inferred from this analysis is shown in Fig. 2 superimposed on the QD image obtained from XSTM measurements of a buried sample.¹⁶

We have determined the in-plane relaxation of QDs by analyzing the in-plane electron density profiles as a function of the distance along the sample normal. These profiles were fit with Gaussians. The half-width at half-maximum (HWHM) of these Gaussians is a result of three contributions that add in quadrature: the experimental broadening resulting from the finite in-plane experimental range in reciprocal space, the thermal Debye–Waller (DW) factors, and the in-plane displacements of the atoms relative to the underlying substrate atoms due to strain. The experimental broadening affects all layers equally and, assuming that the thermal DW factors are also approximately the same, we can remove these contributions using the in-plane HWHM for the substrate. The resulting average in-plane displacement, Δ , is also shown inset in Fig. 1(b) and can be used to calculate the percentage in-plane relaxation, δ_{UC}

$$\delta_{\text{UC}}(z) = \frac{4 * \Delta(z)}{N_{\text{UC}}(z) * a}. \quad (3)$$

Here, $N_{\text{UC}}(z)$ is the number of UCs across a layer at z and a is the GaAs lattice constant. The results are shown inset in Fig. 1(b). Note that even the largest in-plane relaxation 1.07% is much smaller than the mismatch between bulk InAs and GaAs (7%). This means the QDs are almost fully strained all the way to the top of the QD.

Some features of the electron density profiles in Fig. 1 require further explanation. The QD peaks are broader in the vertical direction than the substrate peaks and have a more rectangular shape compared to the Gaussian-like peaks in the substrate. The spacing between the QD peak centers is equal to that of the substrate even though the lattice constant of InAs ($c_{\text{bulk}} = 0.606$ nm) is significantly larger than that of GaAs ($c_{\text{bulk}} = 0.565$ nm). In addition, the entire sequence of QD peak center positions appears to be displaced toward the substrate by about half a UC.

In Fig. 3(a) we present a cut through the electron density which highlights these features, and show a model of the system. The picture that emerges from our direct structure determination is that the QDs sit half a UC (one bilayer) below the uppermost substrate layer [see Fig. 3(c)]. This is consistent with the observation that the QDs nucleate close to bilayer steps.¹³ We also infer from the shape and vertical broadening of the QD peaks that the layers in the QDs exhibit a distinct convex bowing resulting from compressive in-plane stress. The radius of curvature of the layers is esti-

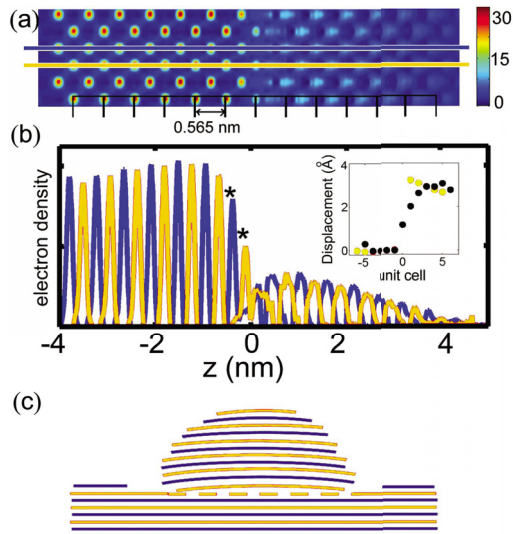


FIG. 3. (Color online) Illustration of the substrate-QD structure. (a) [010] cut through the COBRA-derived electron density map showing G-III atomic positions. The scale bar shows the electron density in units of equivalent electrons. (b) Vertical electron density line profile along the G-III atomic positions indicated by the light and dark lines in (a). The asterisks denote incomplete substrate surface layers. The inset shows the layer positions relative to bulk GaAs determined from COBRA (light) and XSTM (dark). (c) A model of the substrate/QD atomic planes determined from (a) showing the bowed atomic planes within the dot and the displacement of the dot layers by 0.5 UC below the GaAs surface. Note that the horizontal scale in (c) is compressed by a factor of 2 relative to the vertical scale.

mated from the out-of-plane widths of the QD atomic peaks to be $1300 \text{ nm} \pm 20\%$. The atoms on the perimeter of the QDs appear to be at the correct positions predicated by their registry with the substrate surface layer, whereas the bond-lengths of the atoms inside the perimeter of this basal layer are dilated by $\sim 1.5\%$ due to the convex bending.

The inset of Fig. 3(b) shows the displacements of the atoms relative to an ideal GaAs lattice measured using both XSTM and COBRA with good agreement between the two. Both results show a similar shift in layer positions within the dots by about half a UC relative to the substrate layers. The two results cannot be expected to coincide exactly because the XSTM data were obtained on individual QDs while the COBRA data are an average over a very large number of QDs.

In conclusion, the COBRA method reveals details of the composition, atomic structure, and morphology of epitaxial InAs/GaAs QDs that are relevant to their optoelectronic applications. We show that the GaAs (substrate) to InAs (QDs) transition is sharp, occurring within 1–1.5 UCs. Our observations of the substrate-to-QD layer stacking corroborate the role of surface morphology in forming high density QD structures.¹³ We find that the top layer of the substrate is incomplete and apparently indium-free; namely, we do not see any wetting layer. This provides unambiguous, structural

evidence for the transfer of InAs from the wetting layer to the QDs at high coverage.^{17,18} The observed bowing of the atomic layers within the QDs, and consequent dilation at the interface, suggests a partial decoupling of the QDs from the substrate. The detailed results obtained in this work using surface x-ray diffraction and the COBRA method warrant a full theoretical analysis of the underlying electronic energy states leading to the observed atomic structure and the resulting optoelectronic properties of these systems.

This work is supported in part by the Center for Solar and Thermal Energy Conversion, an Energy Frontier Research Center funded by the U.S. Department of Energy, Office of Science, Office of Basic Energy Sciences under Award No. DE-SC00000957. R.C. is supported in part by DOE Grant No. DE-FG02-06ER46273. Use of the Advanced Photon Source at Argonne National Laboratory was supported by the U.S. Department of Energy, Office of Science, Office of Basic Energy Sciences, under Contract No. DE-AC02-06CH11357. VDD and RSG were supported in part by the Department of Energy under Grant No. DE-FG02-06ER46339. JHW was supported by the AFOSR under Contract No. FA9550-06-1-0279 through the MURI program.

¹I. N. Stranski and L. von Krastanow, *Sitzungsber. Akad. Wiss. Wien, Math.-Naturwiss. Kl., Abt. 2B* **146**, 797 (1938).

²A. Yoffe, *Adv. Phys.* **50**, 1 (2001).

³A. Cullis, D. Norris, T. Walther, M. Migliorato, and M. Hopkinson, *Phys. Rev. B* **66**, 081305 (2002).

⁴D. Leonard, K. Pond, and P. Petroff, *Phys. Rev. B* **50**, 11687 (1994).

⁵N. Liu, J. Tersoff, O. Baklenov, A. L. Holmes, Jr., and C. K. Shih, *Phys. Rev. Lett.* **84**, 334 (2000).

⁶P. B. Joyce, T. J. Krzyzewski, G. R. Bell, B. A. Joyce, and T. S. Jones, *Phys. Rev. B* **58**, 5594 (1998).

⁷I. Kegel, T. H. Metzger, A. Lorke, J. Peisl, J. Stangl, G. Bauer, J. M. Garcia, and P. M. Petroff, *Phys. Rev. Lett.* **85**, 1694 (2000).

⁸Y. Yacoby, M. Sowwan, E. Stern, J. Cross, D. Brewster, R. Pindak, J. Pitney, E. M. Dufresne, and R. Clarke, *Nature Mater.* **1**, 99 (2002).

⁹D. P. Kumah, S. Shusterman, Y. Paltiel, Y. Yacoby, and R. Clarke, *Nat. Nanotechnol.* **4**, 835 (2009).

¹⁰D. P. Kumah, A. Ripoan, C. N. Cionca, N. S. Hussein, R. Clarke, J. Y. Lee, J. M. Millunchick, Y. Yacoby, C. M. Schlepuetz, M. Bjoerk, and P. R. Willmott, *Appl. Phys. Lett.* **93**, 081910 (2008).

¹¹M. Geiger, A. Bauknecht, F. Adler, H. Schweizer, and F. Scholz, *J. Cryst. Growth* **170**, 558 (1997).

¹²See supplementary material at <http://dx.doi.org/10.1063/1.3535984> for more details on the sample growth.

¹³W. Ye, S. Hanson, M. Reason, X. Weng, and R. S. Goldman, *J. Vac. Sci. Technol. B* **23**, 1736 (2005).

¹⁴C. Orme, M. D. Johnson, J. L. Sudijono, K. T. Leung, and B. G. Orr, *Appl. Phys. Lett.* **64**, 860 (1994).

¹⁵Y. Yacoby, C. Cionca, N. Hussein, A. Ripoan, J. Olmsted Cross, C. Brooks, D. Schlom, and R. Clarke, *Phys. Rev. B* **77**, 195426 (2008).

¹⁶B. Lita, R. S. Goldman, J. D. Phillips, and P. K. Bhattacharya, *Appl. Phys. Lett.* **74**, 2824 (1999).

¹⁷S. Fafard, Z. R. Wasilewski, and M. Spanner, *Appl. Phys. Lett.* **75**, 1866 (1999).

¹⁸B. Lita, R. S. Goldman, J. D. Phillips, and P. K. Bhattacharya, *Appl. Phys. Lett.* **75**, 2797 (1999).